^{64}Cu-DOTA-Trastuzumab PET Imaging in Patients with HER2-Positive Breast Cancer

Kenji Tamura[1], Hiroaki Kurihara[2], Kan Yonemori[1], Hitoshi Tsuda[3], Junko Suzuki[4], Yuzuru Kono[2], Natsuki Honda[2], Makoto Kodaira[1], Harukaze Yamamoto[1], Mayu Yunokawa[1], Chikako Shimizu[1], Koki Hasegawa[5], Yousuke Kanayama[5], Satoshi Nozaki[5], Takayuki Kinoshita[4], Yasuhiro Wada[5], Shusaku Tazawa[5], Kazuhiro Takahashi[5], Yasuyoshi Watanabe[5], and Yasuhiro Fujiwara[1]

[1]Department of Breast and Medical Oncology, National Cancer Center Hospital, Tokyo, Japan; [2]Department of Diagnostic Radiology, National Cancer Center Hospital, Tokyo, Japan; [3]Department of Pathology and Clinical Laboratories, National Cancer Center Hospital, Tokyo, Japan; [4]Department of Breast Surgery, National Cancer Center Hospital, Tokyo, Japan; and [5]RIKEN Center for Molecular Imaging Science, Hyogo, Japan

The purpose of this study was to determine the safety, distribution, internal dosimetry, and initial human epidermal growth factor receptor 2 (HER2)–positive tumor images of ^{64}Cu-DOTA-trastuzumab in humans. **Methods**: PET was performed on 6 patients with primary or metastatic HER2-positive breast cancer at 1, 24, and 48 h after injection of approximately 130 MBq of the probe ^{64}Cu-DOTA-trastuzumab. Radioactivity data were collected from the blood, urine, and normal-tissue samples of these 6 patients, and the multiorgan biodistribution and internal dosimetry of the probe were evaluated. Safety data were collected for all the patients after the administration of ^{64}Cu-DOTA-trastuzumab and during the 1-wk follow-up period. **Results:** According to our results, the best timing for the assessment of ^{64}Cu-DOTA-trastuzumab uptake by the tumor was 48 h after injection. Radiation exposure during ^{64}Cu-DOTA-trastuzumab PET was equivalent to that during conventional ^{18}F-FDG PET. The radioactivity in the blood was high, but uptake of ^{64}Cu-DOTA-trastuzumab in normal tissues was low. In 2 patients, ^{64}Cu-DOTA-trastuzumab PET showed brain metastases, indicative of blood–brain barrier disruptions. In 3 patients, ^{64}Cu-DOTA-trastuzumab PET imaging also revealed primary breast tumors at the lesion sites initially identified by CT. **Conclusion:** The findings of this study indicated that ^{64}Cu-DOTA-trastuzumab PET is feasible for the identification of HER2-positive lesions in patients with primary and metastatic breast cancer. The dosimetry and pharmacologic safety results were acceptable at the dose required for adequate PET imaging.

Key Words: HER2-positive breast cancer; trastuzumab; PET; ^{64}Cu; molecular imaging

J Nucl Med 2013; 54:1869–1875
DOI: 10.2967/jnumed.112.118612

The discovery of novel molecular targets for anticancer treatment has led to the development of several therapeutic antibodies. Molecular imaging using radiolabeled antibodies can noninvasively identify the presence of specific targets throughout the body. Trastuzumab, a humanized monoclonal antibody against human epidermal growth factor receptor 2 (HER2), is widely used as a standard treatment for HER2-positive breast cancer.

Targeting of HER2 with the monoclonal antibody trastuzumab is a well-established therapeutic strategy for HER2-positive breast cancer in neoadjuvant (*1*), adjuvant (*2,3*), and metastatic settings (*4,5*). Although HER2 expression is routinely determined using immunohistochemistry or FISH (*6*), technical problems can arise when lesions cannot be easily accessed by core-needle biopsy (*7*). In addition, HER2 expression can vary during the course of the disease (*8*) and even across tumor lesions within the same patient (*9*). Therefore, to overcome these problems, a novel technique such as PET molecular imaging is required for the noninvasive evaluation of HER2 expression.

Recently, several novel HER2 inhibitors have been developed, including lapatinib (*10,11*), a HER2 tyrosine kinase inhibitor, which has already been approved for relapsed HER2-positive breast cancer. Pertuzumab, a novel anti-HER2 humanized monoclonal antibody that inhibits receptor dimerization, has a mechanism of action that is complementary to that of trastuzumab. The combination of pertuzumab plus trastuzumab plus docetaxel as first-line treatment significantly prolonged progression-free survival, compared with placebo plus trastuzumab plus docetaxel (*12*). And progression-free and overall survival were significantly longer with trastuzumab emtansine, an antibody drug conjugate, than with lapatinib plus capecitabine after previous treatment with trastuzumab and a taxane (*13*). In contrast, some reports also suggest the efficacy of continuing trastuzumab after progression of metastatic breast cancer. Thus, monitoring the changes in HER2 expression in primary tumor and metastatic sites throughout the course of the disease might be helpful to determine the kind of HER2 inhibitors, or other non-HER2 inhibitors, that should be used in the different phases of treatment.

SPECT was initially used as a noninvasive imaging technique for HER2 (*14,15*). One study reported that SPECT with ^{111}In-labeled trastuzumab found new HER2-positive metastatic lesions (*15*). This finding indicates that SPECT is potentially valuable as a clinical diagnostic tool, although this method does have limitations such as spatial resolution or sensitivity in deep tissues.

To overcome these issues, ^{124}I- and ^{89}Zr-labeled antibody/PET was evaluated in HER2-positive breast cancer (*16–18*). The first

Received Dec. 14, 2012; revision accepted May 9, 2013.
For correspondence or reprints contact: Hiroaki Kurihara, Department of Diagnostic Radiology, National Cancer Center Hospital, 5-1-1 Tsukiji, Chuo-ku, Tokyo 104-0045, Japan.
E-mail: hikuriha@ncc.go.jp
Published online Sep. 12, 2013.

clinical trial using an ^{89}Zr-labeled antibody was performed with U36, a chimeric monoclonal antibody, in head and neck squamous cell carcinoma patients (*19*). Next, an ^{89}Zr-trastuzumab PET trial was conducted in metastatic HER2-positive breast cancer patients (*20*). ^{89}Zr-trastuzumab PET allowed better visualization and semiquantification of uptake in HER2-positive lesions. Unfortunately, ^{111}In, ^{124}I, and ^{89}Zr-trastuzumab, because of their long half-life (67.9, 100.2, and 78.4 h, respectively), resulted in high radiation exposure in patients. For example, the radiation doses of ^{111}In-trastuzumab, ^{124}I-antibody, and ^{89}Zr-trastuzumab were 22, 24, and 18 mSv, respectively, which are 2.5 times higher than that of ^{18}F-FDG PET (*20–22*). In contrast, the half-life of ^{64}Cu is 12.7 h (*23*), suggesting that ^{64}Cu-DOTA-trastuzumab PET could potentially achieve adequate tumor-tissue contrast with high resolution and low radiation exposure because of the shorter half-life of the radioisotope.

In the current study, we attempted to produce good-manufacturing-practice–level ^{64}Cu-labeled trastuzumab with high specific radioactivity and to perform PET imaging with labeled antibodies not only for the detection of primary HER2-positive breast cancer but also for metastatic HER2-positive lesions.

In this clinical study, we evaluated the feasibility and plausible conditions for ^{64}Cu-DOTA-trastuzumab PET imaging for the visualization and quantification of HER2-positive lesions in patients with HER2-positive breast cancer.

MATERIALS AND METHODS

General

All chemical reagents were obtained from commercial sources. This study was conducted according to a protocol approved by the institutional review board and an independent ethics committee of National Cancer Center Hospital. All patients signed a written informed consent form.

Preparation of ^{64}Cu-DOTA-Trastuzumab

^{64}Cu was produced from ^{64}Ni metal powder (ISOFLEX USA) as described previously (*24*). Briefly, the ^{64}Ni (p, n) ^{64}Cu nuclear reaction was performed with 12-MeV proton irradiation using a small medical cyclotron (HM-12S; Sumitomo Heavy Industries. Ltd.). The beam current used was approximately 20 μA (3 h). Trastuzumab IgG (Herceptin; Chugai Pharmaceutical Co., Ltd.) was purified by ultrafiltration (Ultra 0.5 ml 50 k; Amicon) with phosphate-buffered saline (Nacalai Tesque). The obtained trastuzumab (592 μg, 4 nmol) in phosphate-buffered saline (552 μL) was added to 0.16 μg (400 nmol) of DOTA mono *N*-hydroxysuccinimide ester (Macrocyclics Inc.) and dissolved in water for injection (40 μL). After 3 h, crude DOTA-trastuzumab was purified with phosphate-buffered saline using a PD-10 column. The phosphate-buffered saline buffer, including DOTA-trastuzumab (100 μg, 0.7 nmol), was exchanged for a sodium acetate buffer (100 mM, pH 6.5) by filtration.

^{64}Cu-DOTA-trastuzumab injection was prepared by adding $^{64}CuCl_2$ (400–800 MBq; specific activity, 300–2,500 GBq/μmol) to acetate buffer (pH 6.5) solution containing DOTA-trastuzumab and incubating the solution for 1 h at 40°C. The reaction mixture was sterilized by filtration through a 0.22-μm Millex GV filter (Merck Millipore). All the procedures were performed under laminar airflow (class 100 air). The radiolabeling results revealed that the specific activity and radiochemical purity were approximately 350 GBq/μmol and 98%, respectively. Approximately 500 MBq of the final product were obtained by a single radiosynthesis.

^{64}Cu-DOTA-trastuzumab injections passed quality control testing against the following specifications: radioactivity (>150 MBq), volume (3–4 mL), clarity (clear), color (none), pH (6–8), radiochemical purity (>95%), protein abundance (<100 μg), specific activity (>100 GBq/μmol), sterility (Japanese Pharmacopoeia), and endotoxin (<0.25 EU/mL). HER2 immunoreactivities (dissociation constants) of the final products were determined to be approximately 1 nM, as described previously (*25*), using a quartz-crystal microbalance (QCM, single Q0500; SCINICS) with analysis software (QCM1-2, version 1.22; SCINICS).

Patients

Patients included in this study had histologically confirmed invasive HER2-positive (immunohistochemistry 3+ or fluorescence in situ hybridization [FISH]–positive) breast carcinoma, at least 1 site of measurable disease, an Eastern Cooperative Oncology Group performance status of 0–1, and adequate organ function (neutrophil count ≥ 1,500/μL, platelet count ≥ 75,000/μL, hemoglobin concentration ≥ 9.0 g/dL, serum bilirubin ≤ 1.5 mg/dL, aspartate aminotransferase and alanine aminotransferase ≤ 100 IU/L, serum creatinine ≤ 1.5 mg/dL, baseline left ventricular ejection fraction > 60%) and were aged between 20 and 75 y. The main exclusion criteria were congestive heart failure, uncontrolled angina pectoris, arrhythmia, symptomatic infectious disease, severe bleeding, pulmonary fibrosis, obstructive bowel disease or severe diarrhea, symptomatic peripheral or cardiac effusion, and symptomatic brain metastasis.

PET Scanner and Protocol

Images were acquired with a Discovery 600 scanner (GE Healthcare). First, a scout image was acquired to determine the scanning field of the patient, using settings of 10 mA and 120 kV. Next, whole-body 16-slice helical CT and whole-body 3-dimensional PET acquisition were performed. For the whole-body PET/CT study, the scanning field ranged from head to foot. PET images were acquired at 14–16 bed positions with a 2- to 10-min acquisition per bed position, so that they covered the same field as that of whole-body CT. The acquired data were reconstructed as 192 × 192 matrix images (3.65 × 3.65 mm) using a 3-dimensional ordered-subsets expectation maximization algorithm (VUE Point Plus [GE Healthcare]; 32 iterations, 1 subset, and a postprocessing filter of 5 mm in full width at half maximum). PET image evaluation and quantification of the standardized uptake value (SUV) were performed using AW Volume Share 4.5 software (GE Healthcare). Regions of interest were delineated on the PET/CT images, and the maximum SUV was determined.

Safety Monitoring

All patients had received intravenous injections of ^{64}Cu-DOTA-trastuzumab. After the injection, all patients were monitored for 30 min to detect any infusion-related anaphylactic reactions or adverse events. Safety data, including the recording of adverse events, changes in vital signs, physical examination findings, electrocardiogram findings, and laboratory parameters, were collected for all the patients after administration of ^{64}Cu-DOTA-trastuzumab and throughout the 1-wk follow-up period. During PET/CT scanning procedures, vital signs, including blood pressure, temperature, and respiratory rate, were closely monitored and recorded.

Assessment of Feasibility

The whole-body PET/CT study was performed on 6 patients, and sets of images were collected at 1, 24, and 48 h after the injection to evaluate radioactivity distribution, internal dosimetry, and radiation exposure. The internal radiation dose was calculated on the basis of radioactivity data from blood, urinary excretion, and normal tissues of the heart, liver, spleen, kidneys, and other parts of the body at each time point using the OLINDA/EXM software (*26*).

To minimize radiation exposure and contamination of patients, visitors, and health care providers, a radiation survey of each of the

TABLE 1
Patient Characteristics

Patient no.	Age (y)	Histology	Stage	HER2 expression (FISH score)	Interval from CNB to ^{64}Cu (mo)	Primary or metastatic size (cm) or location	No. of lesions visualized by MR imaging/CT/^{64}Cu	History of trastuzumab treatment	Days from trastuzumab treatment to imaging
1	73	IDC-st	IV	3+	20	M, brain	6/4/4	Weekly	1 d
2	42	IDC-SC	IIB	3+	11	P, 2.3 × 2.1	NA/1/1	Triweekly	20 d
3	49	Lobular	IIA	2+ (3.9)	3	P, 2.0 × 2.0	NA/1/1	—	—
4	75	IDC-SC	IV	3+	10	M, brain	1/0/1	Weekly	1 d
5	55	IDC-st	IIA	3+	22	P, 3.5 × 3.5	NA/1/1	Triweekly	8 d
6	45	IDC-SC	IV	3+	1	M, hilar node	NA/1/1	—	—

CNB = core-needle biopsy; ^{64}Cu = ^{64}Cu-DOTA-trastuzumab PET; IDC-st = invasive ductal carcinoma–solid tubular; IDC-SC= invasive ductal carcinoma–scirrhous; M = metastatic breast cancer; P = primary breast cancer; NA = not applied within 1 mo before or after ^{64}Cu-DOTA-trastuzumab PET imaging; weekly = 2 mg/kg/wk; triweekly = 8 mg/kg/3 wk.

6 patients and the patient's room was performed by collecting radioactivity data from the excreted urine, clothes, and linens from days 1–3 in the administrative area for radiotherapy at the National Cancer Center Hospital. The radiation dose rate was also evaluated at a distance of 1 m from the surface of each patient by a survey meter, immediately after the injection of ^{64}Cu-DOTA-trastuzumab, to confirm the feasibility of using ^{64}Cu-DOTA-trastuzumab PET/CT for outpatients.

RESULTS

Patient Characteristics

Between December 2010 and November 2011, 6 patients were enrolled in the current study. Patient characteristics are presented in Table 1. The median age of the patients was 58 y. The histologic type for almost all tumors was invasive ductal breast carcinoma, either solid tubular or scirrhous type. There was 1 lobular breast carcinoma. Five patients (83%) had HER2-positive tumors that were immunohistochemistry 3+, whereas 1 patient (17%) had HER2-positive tumors that were both immunohistochemistry 2+ and FISH-positive. Three primary cancers in stage IIA–IIB and 3 metastatic cancers with brain and hilar node metastases were detected. No infusion-related reactions or adverse events were observed during the study.

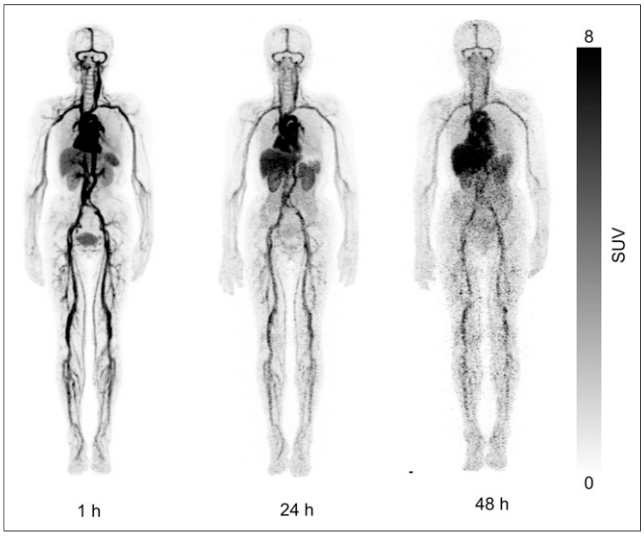

FIGURE 1. Whole-body ^{64}Cu-DOTA-trastuzumab PET images at 1, 24, and 48 h after injection (patient 4).

Injection Dose and Safety Monitoring

The mean and SD of the administered mass of ^{64}Cu-DOTA-trastuzumab was 86.2 ± 6.3 μg (range, 80.6–91.8 μg). The mean administered activity was 126 ± 8 MBq (range, 115–136 MBq). The administration of ^{64}Cu-DOTA-trastuzumab was well tolerated by all subjects. No drug-related adverse events were reported for any of the patients included in this study. No clinically important trends indicative of a safety signal were noted for the laboratory parameters, vital signs, or electrocardiogram parameters.

Conditions for Imaging

The whole-body distribution of ^{64}Cu-DOTA-trastuzumab in patient 4 is shown in Figure 1. Figure 2A shows typical decay-corrected time–activity curves for normal organ tissue at 1, 24, and 48 h after the injection for all 6 patients. Whole-body SUV was relatively stable, in the range of 0.8–1.0. SUV in blood at 1, 24, and 48 h after the injection showed high values of 8.3–11.1, 4.5–8.1, and 3.3–6.4, respectively. In contrast, SUV in the urinary bladder showed a rapid decrease approximately 24 h after the injection. The radioactivity voided into urine within 1 h after injection ranged from 2% to 5% of the injected activity, which was similar to the percentages of unlabeled ^{64}Cu in the injected activity (Supplemental Table 1; supplemental materials are available at http://jnm.snmjournals.org). Biodistribution in the liver, spleen, and kidney was as expected for these well-perfused organs. The radioactivity in the liver was higher in patients 3 and 6, who had no history of trastuzumab treatment, than in the other patients. The target tumor uptake showed better contrast at 48 h after the injection than at 24 h after the injection (Fig. 2B). These findings indicate that the plausible timing for imaging in this series of measurement is 48 h after injection of ^{64}Cu-DOTA-trastuzumab.

Assessment of Feasibility

Internal dosimetry was evaluated in all 6 patients. The target radioactivity was 150 MBq, and the average radioactivity for the 6 patients was 126 MBq. The organ-absorbed and effective doses are shown in Table 2. The highest absorbed dose was in the heart wall, followed by the liver, spleen, and kidneys. The average of the effective dose was estimated to be 0.036 ± 0.009 mSv/MBq.

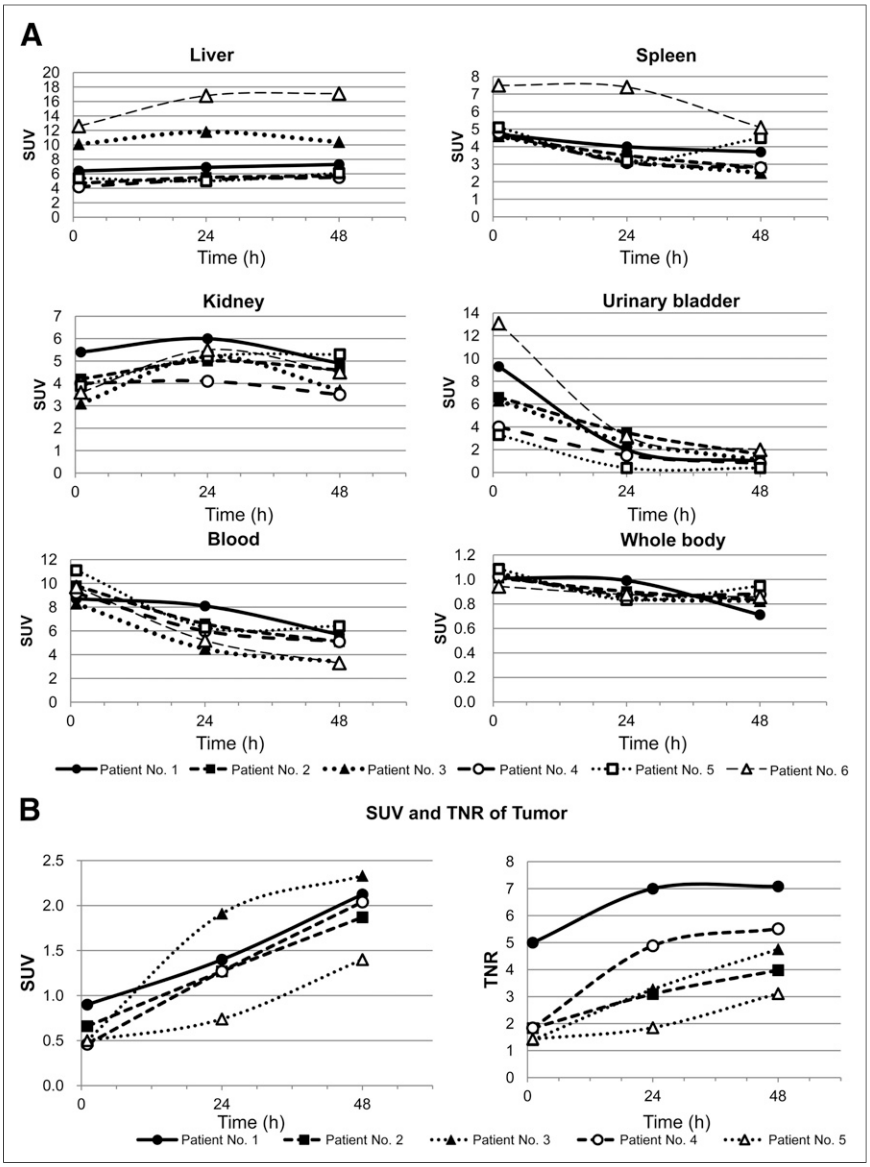

FIGURE 2. Regional time–activity curves of ^{64}Cu-DOTA-trastuzumab in 6 patients. (A) SUVs in blood, urinary bladder, liver, kidney, spleen, and whole body were calculated from region-of-interest–based analysis for each tissue. SUV in blood was measured from region of interest of heart content. (B) SUVs in tumor and tumor-to-normal tissue ratio (TNR) were also calculated. In patient 6, SUV in tumor and TNR could not be calculated because of nonspecific high uptake of ^{64}Cu-DOTA-trastuzumab within heart and large vessels.

Patient radiation surveys, conducted using a survey meter, revealed that the radiation dose rate at 1 m from the surface of each patient immediately after the injection of ^{64}Cu-DOTA-trastuzumab was approximately 7–10 (μSv/h). The average decay-corrected radioactivity in urine samples collected within 24 h after injection of the probe was approximately 4.2 MBq (Table 3, urinary excretion). Radioactivity in urine samples obtained on days 2 and 3 decreased to less than 1 MBq. Radiation surveys of patient rooms revealed that the radioactivity of clothes and linens was at background levels.

Initial Analysis of Tumor PET Image with ^{64}Cu-DOTA-Trastuzumab

Most of the HER2-positive lesions previously identified by CT, MR imaging, or bone scans could also be seen on the ^{64}Cu-DOTA-trastuzumab PET scan at 48 h after the injection. In this pilot study, primary breast tumors that had been identified as HER2-positive by immunohistochemistry and FISH were clearly visualized by ^{64}Cu-DOTA-trastuzumab PET imaging in 3 patients (Fig. 3). The smallest primary breast carcinoma lesion revealed by ^{64}Cu-DOTA-trastuzumab PET imaging measured 2.0 × 2.0 cm on breast sonography (Table 1). Brain metastases were also visualized by ^{64}Cu-DOTA-trastuzumab PET in 2 patients. In patient 1, with multiple brain metastases in the cerebellar hemisphere, the PET scan showed ^{64}Cu-DOTA-trastuzumab accumulation in lesions that corresponded to those observed on MR imaging (Fig. 4A). In patient 4, ^{64}Cu-DOTA-trastuzumab PET imaging could detect a solitary brain metastasis that had been identified in a similar location by MR imaging (Fig. 4B). A hilar lymph node metastasis located near the great vessels and heart in patient 6 was not detected by ^{64}Cu-DOTA-trastuzumab PET imaging.

DISCUSSION

This study, performed on humans for—to our knowledge—the first time, revealed that ^{64}Cu-DOTA-trastuzumab PET imaging was safe and feasible even for outpatients and that the estimated effective dose was 0.036 mSv/MBq. The internal radiation dose of ^{64}Cu-DOTA-trastuzumab PET absorbed by the patient was estimated to be 4.5 mSv (0.036 × 126). In contrast, the average effective dose in routine ^{18}F-FDG PET is approximately 0.019 mSv/MBq, and target radioactivity per injection is 370–740 MBq (*27*). Therefore, the internal radiation dose absorbed by the patient per ^{18}F-FDG PET scan was estimated to be 7.0–14 mSv (0.019 × 370–740), indicating that the internal radiation dose of ^{64}Cu-DOTA-trastuzumab PET was lower than that of conventional ^{18}F-FDG PET.

The pilot tumor images of ^{64}Cu-DOTA-trastuzumab PET demonstrated successful tumor uptake and visualization of HER2-positive primary breast carcinoma and metastatic lesions in the brain. High SUV in the heart and blood vessels could reflect the biologic stability of trastuzumab in blood. The balance between the sustained accumulation of ^{64}Cu-DOTA-trastuzumab in the tumors, blood clearance of injected ^{64}Cu-DOTA-trastuzumab, and radioactive decay of ^{64}Cu indicate the plausible timing for imaging. Here, we confirmed that the plausible timing for imaging, using the scanning protocol described in this study, was 48 h after the injection. Compared with an optimal imaging time of 5 d after ^{89}Zr-trastuzumab injection (*20*), ^{64}Cu-DOTA-trastuzumab seems to be more acceptable in clinical practice. The radiation exposure per injection in a patient receiving ^{64}Cu-DOTA-trastuzumab PET was estimated to be 4.5 mSv, which is

TABLE 2
Organ-Absorbed Dose and Effective Dose Estimated from Whole-Body ^{64}Cu-DOTA-Trastuzumab PET

Organ	Absorbed dose (mGy/MBq)
Adrenals	0.031 ± 0.004
Brain	0.015 ± 0.003
Breasts	0.020 ± 0.001
Gallbladder wall	0.035 ± 0.008
LLI wall	0.018 ± 0.002
Small intestine	0.019 ± 0.001
Stomach wall	0.024 ± 0.002
ULI wall	0.022 ± 0.002
Heart wall	0.340 ± 0.046
Kidneys	0.103 ± 0.034
Liver	0.237 ± 0.117
Lungs	0.057 ± 0.070
Muscle	0.023 ± 0.006
Ovaries	0.018 ± 0.002
Pancreas	0.032 ± 0.003
Red marrow	0.017 ± 0.001
Osteogenic cells	0.035 ± 0.001
Skin	0.015 ± 0.001
Spleen	0.142 ± 0.040
Thymus	0.030 ± 0.002
Thyroid	0.016 ± 0.001
Urinary bladder wall	0.023 ± 0.006
Uterus	0.018 ± 0.002
Total body	0.029 ± 0.004

LLI = lower large intestine; ULI = upper large intestine.
Effective dose = 0.036 ± 0.009 mSv/MBq.

much lower than that of ^{89}Zr-trastuzumab PET (18 mSv) (*20*). These findings confirm the feasibility of this novel PET imaging method even in an outpatient setting based on the shorter half-life of this isotope relative to ^{111}In, ^{124}I, and ^{89}Zn. Thus, there are likely benefits and drawbacks to each of these compounds. Because of its relatively longer half-life, allowing the patient to be imaged at longer time points, ^{89}Zn-trastuzumab provides clearer images; however, it induces higher radiation exposure. On the other hand, the shorter half-life of ^{64}Cu induces lower radiation exposure; however, it provides images with nonspecific activity in the blood. It was difficult to detect lesions around the liver, heart, and blood because of the nonspecific high uptake of the probe within these organs, which is considered a disadvantage of this method. One possible approach to decreasing the nonspecific background is to use ^{64}Cu-DOTA-trastuzumab F(ab′)$_2$ fragments (*28*). The small, molecule-sized, antibody fragment probe might achieve rapid clearance from the blood resulting in better target detection. We are currently trying to downsize the antibody molecules, but thus far, the affinity of F(ab′)$_2$ fragments has been much less than that of the original full-sized antibody. Another possible approach to decreasing high uptake of the probe by the liver could be to use cold trastuzumab with ^{64}Cu-DOTA-trastuzumab injection. The relatively high uptake by the liver in patients 3 and 6, who had no history of trastuzumab therapy, may suggest the effectiveness of using cold trastuzumab. An adequate interval from predosing of the cold trastuzumab should be determined in a future study. Moreover, the cutoff level must be precisely addressed to discriminate between normal tissues and HER2-positive tumors in larger sample sizes.

An interesting finding of this study was that ^{64}Cu-DOTA-trastuzumab could target brain metastatic lesions. In a clinical setting, it is not possible to obtain a brain tissue sample without surgery; however, knowledge of the HER2 status would in turn allow the identification of the best additional systemic treatment to control the symptoms of the central nervous system. Although penetration of the blood–brain barrier by trastuzumab is generally considered to be poor, we could visualize brain lesions in this study, probably because of disruption of the blood–brain barrier at the site of brain metastasis or whole-brain radiation. PET imaging with ^{64}Cu-DOTA-trastuzumab may have potential to characterize the HER2 status of brain lesions, but further study of both HER2-positive and HER2-negative tumors is necessary.

A potential application of ^{64}Cu-DOTA-trastuzumab PET imaging may lie in its ability to allow for the initial evaluation of the HER2 status of tumors by a means other than biopsy. We successfully detected primary HER2-positive breast tumors in 3 patients using this technique. However, further studies are needed to find the relative sensitivity and specificity of this imaging technique by comparison with conventional immunohistochemistry or FISH testing.

Another potential application of ^{64}Cu-DOTA-trastuzumab PET imaging is in the biologic monitoring of HER2 expression during the course of the disease. Differences in HER2 expression within the same patient across a tumor lesion or at different periods have

TABLE 3
Injected Radioactivity and Effective Dose for 6 Patients and Radiation Survey for Each Patient and Patient Room

Parameter	Patient no.					
	1	2	3	4	5	6
Injected radioactivity (MBq)	136	119	115	129	134	124
Effective dose* (mSv/MBq)	0.050	0.029	0.035	0.028	0.028	0.043
Dose rate at 1 m (μSv/h)†	10	8	7	10	11	8
Urinary excretion, day 1 (MBq)	3.1	7.2	2.4	3.2	3.7	5.8
Urinary excretion, day 2 (MBq)	0.44	0.29	0.30	0.36	0.57	0.61
Clothes, linens, day 2 (MBq)	BG	BG	BG	BG	BG	BG
Urinary excretion, day 3 (MBq)	0.30	0.15	0.26	0.11	0.33	0.16
Clothes, linens, day 3 (MBq)	BG	BG	BG	BG	BG	BG

*Average of effective dose was 0.036 mSv/MBq.
†Radiologic dose rate measured at 1 m from surface of patient.
BG = background level.

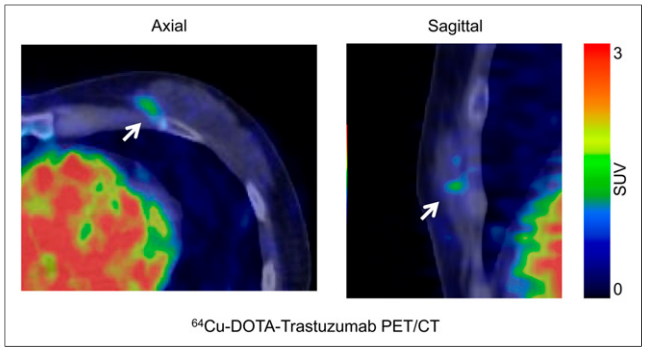

FIGURE 3. ^{64}Cu-DOTA-trastuzumab PET images of HER2-positive primary breast tumor. Arrows show primary breast tumor in patient 3. Red regions indicate high uptake ^{64}Cu-DOTA-trastuzumab in heart and blood vessels.

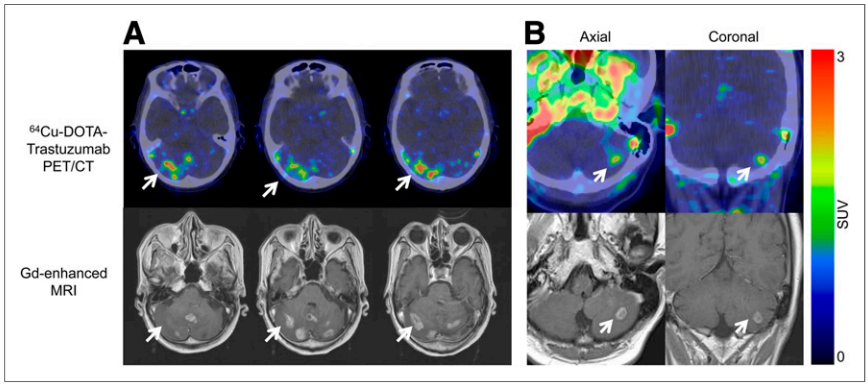

FIGURE 4. ^{64}Cu-DOTA-trastuzumab PET images of HER2-positive metastatic brain lesions (arrows). (A) Brain metastases were clearly visualized by ^{64}Cu-DOTA-trastuzumab PET in patient 1. Significant uptake values were found in areas corresponding to brain metastatic lesions that were detected by MR imaging. Some brain metastases could not be detected on conventional CT. (B) In patient 4, ^{64}Cu-DOTA-trastuzumab PET imaging could detect solitary brain metastasis that had also been identified in similar location by MR imaging.

been reported (*8,9*). ^{64}Cu-DOTA-trastuzumab PET imaging is associated with a potent quantitative biomarker that can predict the biologic effect of anti-HER2 antibodies. This information might help in the choice between anti-HER2 antibodies (*4,12,29*) and HER2 tyrosine kinase inhibitors (*10,11*) for individual HER2 inhibitor therapy.

In addition to these 2 applications in breast cancer patients, ^{64}Cu-DOTA-trastuzumab PET imaging may also be applicable in other kinds of malignancies. Trastuzumab in combination with chemotherapy can be considered a new standard option for patients with HER2-positive advanced gastric cancer (*30*). Consequently, ^{64}Cu-DOTA-trastuzumab PET imaging in gastric cancer is an expanding area of research.

In this study, the time from biopsy to ^{64}Cu-DOTA-trastuzumab PET imaging ranged from 1 to 22 mo, and most of these individuals received trastuzumab therapy during these periods. HER2 status may change over time and with anti-HER therapy; however, we could not confirm the HER2 status at the time of ^{64}Cu-DOTA-trastuzumab PET imaging. This is a potential weakness of our study, but in general, it is difficult to assess the biologic specificity of HER2 PET in humans because of the need for an additional biopsy after the administration of the probe. In a xenografted model using tumors with 2 different HER2 expression levels, we have confirmed the HER2 specificity of ^{64}Cu-DOTA-trastuzumab PET imaging (Supplemental Fig. 1). To confirm the HER2 specificity of ^{64}Cu-DOTA-trastuzumab PET imaging in humans, further studies are required to compare the results of pathologic studies performed after surgery or core-needle biopsy with the HER2 status obtained on PET.

CONCLUSION

^{64}Cu-labeled molecular target probes may allow rapid evaluation during early screening of leading compounds in preclinical studies and in the development of anticancer drugs. In clinical studies, these probes also have great potential to achieve proof of concept. In combination with pharmacokinetic and pharmacodynamic studies, molecular imaging studies in a clinical trial would provide a more powerful approach to explore appropriate ways of using molecule-targeted drugs.

DISCLOSURE

The costs of publication of this article were defrayed in part by the payment of page charges. Therefore, and solely to indicate this fact, this article is hereby marked "advertisement" in accordance with 18 USC section 1734. This study was supported by a consignment expense for the Japan Advanced Molecular Imaging Program (JAMP) from the Ministry of Education, Culture, Sports, Science and Technology (MEXT), Japanese Government. No other potential conflict of interest relevant to this article was reported.

ACKNOWLEDGMENTS

We thank Chinuyo Sumita, Riyo Zochi, Yoko Morimoto, and the staff of the RIKEN Center for Molecular Imaging Science for supplying ^{64}Cu-DOTA-trastuzumab and their technical support. We also thank Nao Nakamura and Rumi Koyama for secretarial support during this study. Finally, we thank all the study participants and patients who provided tissue samples for this analysis.

REFERENCES

1. Buzdar AU, Ibrahim NK, Francis D, et al. Significantly higher pathologic complete remission rate after neoadjuvant therapy with trastuzumab, paclitaxel, and epirubicin chemotherapy: results of a randomized trial in human epidermal growth factor receptor 2–positive operable breast cancer. *J Clin Oncol.* 2005;23:3676–3685.
2. Piccart-Gebhart MJ, Procter M, Leyland-Jones B, et al.; Herceptin Adjuvant (HERA) Trial Study Team. Trastuzumab after adjuvant chemotherapy in HER2-positive breast cancer. *N Engl J Med.* 2005;353:1659–1672.
3. Romond EH, Perez EA, Bryant J, et al. Trastuzumab plus adjuvant chemotherapy for operable HER2-positive breast cancer. *N Engl J Med.* 2005;353:1673–1684.
4. Slamon DJ, Leyland-Jones B, Shak S, et al. Use of chemotherapy plus a monoclonal antibody against HER2 for metastatic breast cancer that overexpresses HER2. *N Engl J Med.* 2001;344:783–792.
5. Tripathy D, Slamon DJ, Cobleigh M, et al. Safety of treatment of metastatic breast cancer with trastuzumab beyond disease progression. *J Clin Oncol.* 2004;22:1063–1070.
6. Sauter G, Lee J, Bartlett JM, Slamon DJ, Press MF. Guidelines for human epidermal growth factor receptor 2 testing: biologic and methodologic considerations. *J Clin Oncol.* 2009;27:1323–1333.

7. Lebeau A, Turzynski A, Braun S, et al. Reliability of human epidermal growth factor receptor 2 immunohistochemistry in breast core needle biopsies. *J Clin Oncol.* 2010;28:3264–3270.
8. Xiao C, Gong Y, Han EY, Gonzalez-Angulo AM, Sneige N. Stability of HER2-positive status in breast carcinoma: a comparison between primary and paired metastatic tumors with regard to the possible impact of intervening trastuzumab treatment. *Ann Oncol.* 2011;22:1547–1553.
9. Houssami N, Macaskill P, Balleine RL, Bilous M, Pegram MD. HER2 discordance between primary breast cancer and its paired metastasis: tumor biology or test artifact? Insights through meta-analysis. *Breast Cancer Res Treat.* 2011; 129:659–674.
10. Geyer CE, Forster J, Lindquist D, et al. Lapatinib plus capecitabine for HER2-positive advanced breast cancer. *N Engl J Med.* 2006;355:2733–2743.
11. Blackwell KL, Burstein HJ, Storniolo AM, et al. Randomized study of Lapatinib alone or in combination with trastuzumab in women with ErbB2-positive, trastuzumab-refractory metastatic breast cancer. *J Clin Oncol.* 2010;28:1124–1130.
12. Baselga J, Cortés J, Kim SB, et al.; CLEOPATRA Study Group. Pertuzumab plus trastuzumab plus docetaxel for metastatic breast cancer. *N Engl J Med.* 2012; 366:109–119.
13. Verma S, Miles D, Gianni L, et al.; EMILIA Study Group. Trastuzumab emtansine for HER2-positive advanced breast cancer. *N Engl J Med.* 2012;367:1783–1791.
14. de Korte MA, de Vries EG, Lub-de Hooge MN, et al. ^{111}Indium-trastuzumab visualises myocardial human epidermal growth factor receptor 2 expression shortly after anthracycline treatment but not during heart failure: a clue to uncover the mechanisms of trastuzumab-related cardiotoxicity. *Eur J Cancer.* 2007;43:2046–2051.
15. Perik PJ, Lub-De Hooge MN, Gietema JA, et al. Indium-111-labeled trastuzumab scintigraphy in patients with human epidermal growth factor receptor 2-positive metastatic breast cancer. *J Clin Oncol.* 2006;24:2276–2282.
16. Robinson MK, Doss M, Shaller C, et al. Quantitative immuno-positron emission tomography imaging of HER2-positive tumor xenografts with an iodine-124 labeled anti-HER2 diabody. *Cancer Res.* 2005;65:1471–1478.
17. Reddy S, Shaller CC, Doss M, et al. Evaluation of anti-HER2 C6.5 diabody as a PET radiotracer to monitor HER2 status and predict response to trastuzumab treatment. *Clin Cancer Res.* 2011;17:1509–1520.
18. Oude Munnink TH, Korte MA, Nagengast WB, et al. ^{89}Zr-trastuzumab PET visualises HER2 down regulation by the HSP90 inhibitor NVP-AUY922 in a human tumor xenograft. *Eur J Cancer.* 2010;46:678–684.
19. Börjesson PK, Jauw YW, Boellaard R, et al. Performance of immuno–positron emission tomography with zirconium-89-labeled chimeric monoclonal antibody U36 in the detection of lymph node metastases in head and neck cancer patients. *Clin Cancer Res.* 2006;12:2133–2140.
20. Dijkers EC, Oude Munnink TH, Kosterink JG, et al. Biodistribution of ^{89}Zr-trastuzumab and PET imaging of HER2-positive lesions in patients with metastatic breast cancer. *Clin Pharmacol Ther.* 2010;87:586–592.
21. Kurdziel K, Mena E, Adler S, et al. Human dosimetry and tumor kinetics of ^{111}In CHX-A" DTPA trastuzumab in solid tumors using gamma-camera imaging [abstract]. *J Nucl Med.* 2011;52(suppl 1):308P.
22. Jayson GC, Zweit J, Jackson A, et al. Molecular imaging and biological evaluation of HuMV833 anti-VEGF antibody: implications for trial design of anti-angiogenetic antibodies. *J Natl Cancer Inst.* 2002;94:1484–1493.
23. Li ZB, Niu G, Wang H, et al. Imaging of urokinase-type plasminogen activator receptor expression using a ^{64}Cu-labeled linear peptide antagonist by microPET. *Clin Cancer Res.* 2008;14:4758–4766.
24. Obata A, Kasamatsu S, McCarthy DW, et al. Production of therapeutic quantities of ^{64}Cu using a 12 MeV cyclotron. *Nucl Med Biol.* 2003;30:535–539.
25. Iijima M, Kadoya H, Hatahira S, et al. Nanocapsules incorporating IgG Fc-binding domain derived from Staphylococcus aureus protein-A for displaying IgGs on immunosensor chips. *Biomaterials.* 2011;32:1455–1464.
26. Stabin MG, Sparks RB, Crowe E. OLINDA/EXM: the second-generation personal computer software for internal dose assessment in nuclear medicine. *J Nucl Med.* 2005;46:1023–1027.
27. Delbeke D, Coleman RE, Guiberteau MJ, et al. Procedure guideline for tumor imaging with ^{18}F-FDG PET/CT 1.0. *J Nucl Med.* 2006;47:885–895.
28. Leung K. ^{64}Cu-1,4,7,10-tetraazacyclododecane-1,4,7,10-tetraacetic acid-epidermal growth factor receptor-binding fibronectin domain E13.4.3′. Molecular Imaging and Contrast Agent Database (MICAD). http://www.ncbi.nlm.nih.gov/books/NBK99555/. Published May 3, 2013. Updated August 9, 2013. Accessed August 29, 2013.
29. LoRusso PM, Weiss D, Guardino E, Girish S, Sliwkowski MX. Trastuzumab emtansine: a unique antibody-drug conjugate in development for human epidermal growth factor receptor 2-positive cancer. *Clin Cancer Res.* 2011;17:6437–6447.
30. Bang YJ, Van Cutsem E, Feyereislova A, et al. Trastuzumab in combination with chemotherapy versus chemotherapy alone for treatment of HER2-positive advanced gastric or gastro-oesophageal junction cancer (ToGA): a phase 3, open-label, randomised controlled trial. *Lancet.* 2010;376:687–697.